JOURNAL OF MASS SPECTROMETRY, VOL. 32, 1019–1036 (1997)

SPECIAL FEATURE
TUTORIAL

Post-source Decay Analysis in Matrix-assisted Laser Desorption/Ionization Mass Spectrometry of Biomolecules†

Bernhard Spengler*
Institute of Laser Medicine, Heinrich Heine University Düsseldorf, P.O. Box 101007, D-40001 Düsseldorf, Germany

An introduction to primary structure analysis of biomolecules by matrix-assisted laser desorption/ionization (MALDI) post-source decay (PSD) is given, sketching the principles and applications of the method for scientists in molecular biology, biochemistry and biomedicine. The fundamentals of PSD are described in order to explain the potential and limitations of its applicability. Two examples of peptide sequencing of a completely unknown peptide and of a database-listed peptide are presented and the procedure of (non-automated) amino acid sequence elucidation is described. © **1997 by John Wiley & Sons, Ltd.**

J. Mass Spectrom. **32**, 1019–1036 (1997)
No. of Figures: 21 No. of Tables: 1 No. of Refs: 62

KEYWORDS: post-source decay analysis; matrix-assisted laser desorption/ionization mass spectrometry; biomolecules

INTRODUCTION

Mass spectrometric analysis of product ions from post-source decay of precursor ions that were formed by matrix-assisted laser desorption ionization (MALDI-PSD)[1–4] has evolved into a powerful method for primary structure analysis of biopolymers. Especially in the field of peptide sequencing, MALDI-PSD has been widely applied, mainly because of its high sensitivity for prepared sample amounts in the range 30–100 fmol and because of its high tolerance of sample impurities and sample inhomogeneity.[5–12]

Automated Edman degradation as the primary method of peptide sequence analysis is now being increasingly replaced by mass spectrometric (MS) methods[13,14] such as electrospray ionization combined with triple-quadrupole or ion-trap mass spectrometers[15] and by MALDI-PSD. Compared with Edman sequencing, the main advantages of mass spectrometric peptide sequencing are its compatibility with chemical modifications (derivatization, glycosylation, *N*-terminal modification, etc.), its much higher sensitivity and the possibility of analyzing multi-component samples and (especially in the case of MALDI-PSD) just barely purified samples. The simplicity of the instrumentation required for MALDI-PSD (compared with classical four-sector MS/MS instruments or triple-quadrupole instruments) and the simplicity of operation have led to the rapid acceptance of the method and to its broad application in molecular biology.[16–23]

METHODS AND MECHANISMS

Fundamental aspects of ion stability and post-source decay

PSD analysis is an extension of MALDI/MS that allows one to observe and identify structurally informative fragment ions from decay taking place in the field-free region after leaving the ion source.

After the development of MALDI[24–26] as a new and brilliant technique for the analysis of very large biomolecules in the mass range up to more than 100 000 u,

* Correspondence to: B. Spengler, Institute of Laser Medicine, Heinrich Heine University, Düsseldorf, Germany

† **Dedicated to Raimund Kaufmann, born February 14, 1934, died September 1, 1997.**

Contract grant sponsor: Bundesministerium für Bildung, Wissenschaft, Forschung und Technologie (BMBF); *Contract grant number:* 0310709.
Contract grant sponsor: European Community; *Contract grant number:* MAT1-CT94-DO34
Contract grant sponsor: Ministerium für Wissenschaft und Forschung, Nordrhein-Westfalen.
Contract grant sponsor: Thermo Bioanalysis Ltd.

CCC 1076–5174/97/101019–18 $17.50

Received 31 July 1997
Accepted 4 September 1997

it was first concluded that ions formed by this technique must be extremely stable and internally cool and that MALDI is therefore a very 'soft' ionization technique. The main reason for this assumption was that these large molecules could be desorbed and ionized intact (which was impossible with ionization techniques available at that time), that no fragment ions were observed in the spectra apart from the molecular ion signal and that these molecular ions obviously survived hundreds of microseconds during their flight through the instrument until detection. A few unexplained observations, however, puzzled the developers at that time, finally leading to considerable doubts about the general stability of MALDI ions:

- The mass resolving power of MALDI instruments was extremely low at first, not exceeding values of $M/\Delta M$ in the range 30–50 (meaning that neighboring ion signals at 100 000 and 103 000 u remained unresolved). The main limitation of mass resolution was found to be located in the ion detection step,[27] but even taking that into account the remaining peak widths were still too large.
- Scientists developing new MALDI instruments with acceleration voltages higher than that of the original MALDI instrument obtained better results with linear time-of-flight analyzers than with ion reflector analyzers (used for compensation of initial energy distributions).
- Instruments with ion reflectors did not exhibit a higher mass resolving power than linear instruments, even though the former were known to possess a high resolving power with classical ionization techniques.
- A reasonable sensitivity and mass resolving power was found even with a Wiley–McLaren-type time-of-flight mass spectrometer in the very early days of MALDI-MS[28] using orthogonal acceleration and delayed ion extraction with an acceleration voltage of only 150 V and a total ion kinetic energy of only 3000 eV (Fig. 1). If the decrease in mass resolving power was resulting from ion instability, one would suggest that only instruments with high acceleration voltages (short total ion flight times) should give acceptable results, rather than instruments that use free expansion of ions over microseconds before ion acceleration.
- Extremely high energy deficits were observed in ion retarding experiments, which could only be attributed to fragmentation rather than energy loss of stable ions.[29,30]

Retarding field experiments finally could be used to quantify the instability of MALDI-generated ions and characterize its dependence on several instrumental parameters.[3] Using a specially designed deceleration stage in a linear time-of-flight instrument, the flight time of stable molecular ions could be increased at constant flight times of neutral products from the decay of these ions. Analysis of the signal intensities of the two signals from stable ions and from neutral decay products led to the determination of unimolecular decay rates and collision cross-sections as a function of instrumental and methodological parameters. One of the most important parameters for post-source decay was found to be the initial acceleration field. Figure 2 summarizes the behavior for the case of the peptide substance P. The diagram shows the strong increase in the unimolecular rate constant with increasing initial field strength. This behavior directly explains the high sensitivity for large ion detection in the early experiments using a pulsed extraction instrument (Fig. 1) and also the original MALDI instrument employing a comparably low initial acceleration field. The use of zero initial acceleration field leads to a minimized decay rate of ions formed.

The physical reason for the observed dependence of ion stability on the acceleration field strength can be better understood after discussion of another experimental observation. Figure 3 displays an ion density distribution of a neat matrix sample [2,5-dihydroxybenzoic acid (DHB)] and of a typical sample preparation of substance P in DHB matrix. The ion densities were measured by angular resolved time-of-flight detection after field-free expansion of laser-desorbed material. Flight time and mass evaluation allowed us to recalculate, for a given 'snapshot' time, the actual spatial distribution of the ions measured.[31]

The upper image from the neat matrix sample shows a slightly forward peaked distribution with the highest ion densities for the slowest ions. In contrast, the lower image taken from the MALDI preparation of substance P in DHB at a low molar ratio of matrix to analyte shows considerable quenching of the slow matrix ions

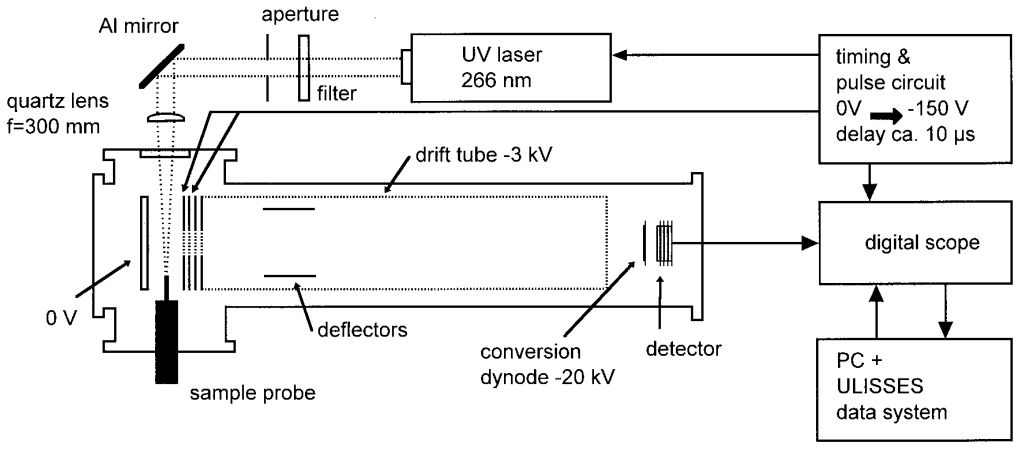

Figure 1. Scheme of an early MALDI mass spectrometer with Wiley–McLaren-type pulsed ion extraction.[28]

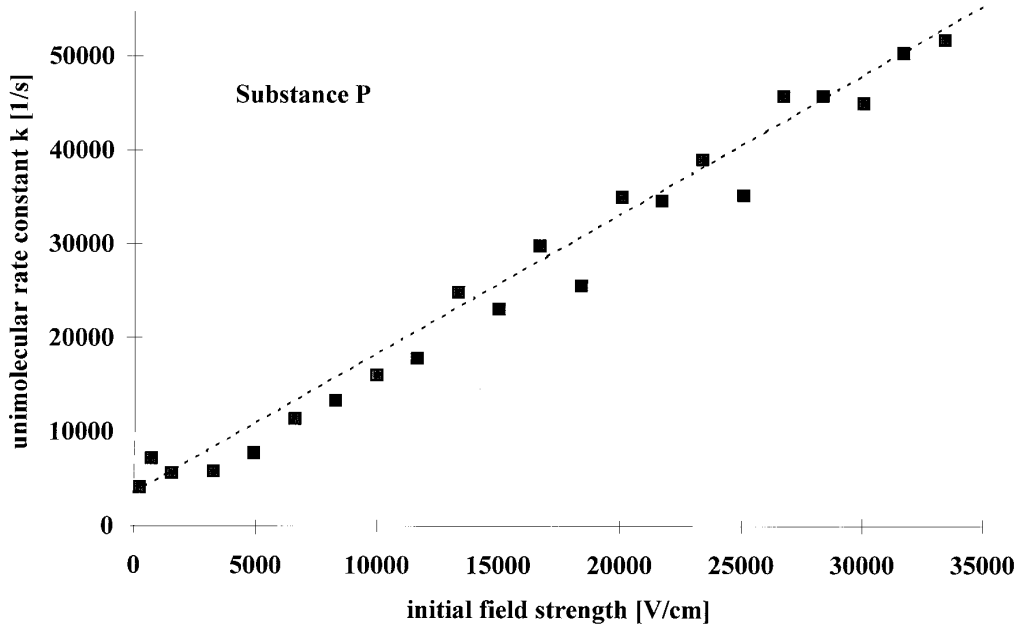

Figure 2. Unimolecular rate constant of peptide ions in the field-free drift region of a linear time-of-flight instrument as a function of the field strength above the sample surface at the laser pulse time. A decay rate about five times lower for the case of a delayed ion extraction (zero initial field) was found, compared with typical conditions of 10 kV cm^{-1} in prompt extraction instruments.

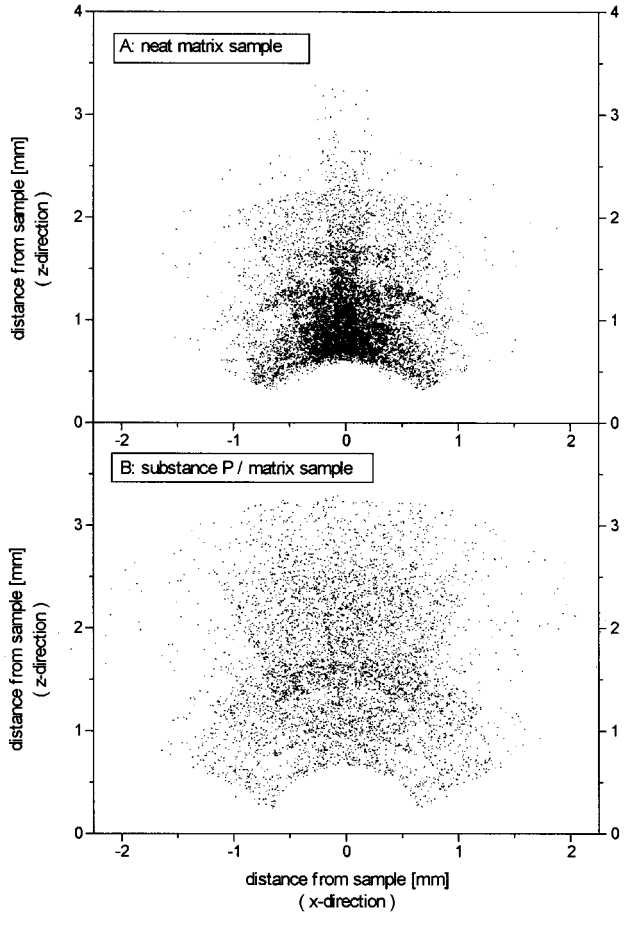

Figure 3. Ion density distribution of matrix and peptide ions above the surface of a MALDI sample 1 μs after the laser shot. (A) Neat matrix sample (dried droplet method) of 2,5-dihydroxybenzoic acid (DHB); (B) substance P prepared in DHB matrix (dried droplet method). Blue dots: matrix ions; Red dots: substance P ions.

(blue dots) that were of high intensity in the measurements of the neat matrix sample. The detected substance P ions instead overlap the region of quenched matrix ions. It is therefore assumed that substance P ions are formed by proton exchange between matrix ions and neutral substance P molecules in the gas phase. The 'overlap model' derived from these measurements[31] helps in understanding the ionization process in MALDI, in explaining the observed energy deficits[32] and surplus energies and in explaining the dependence of ion stability on initial acceleration field strength, as described in the following. It is known from earlier investigations[33] that for smaller molecules of high spectral absorption the number of neutral molecules desorbed by UV laser irradiation is orders of magnitude higher than the number of ionized molecules. The velocity distribution of these neutral molecules is comparable to that observed for their ions. It can therefore be concluded that the cloud of faster matrix ions in Fig. 3(B) in front of the cloud of substance P ions represents a much denser cloud of neutral matrix molecules. By acceleration of the substance P ions through this cloud of neutral matrix molecules, a large number of collisions take place, leading to a considerable increase in internal energy (and thus instability) of the analyte ions. The increase in fragmentation rate with increasing initial acceleration field strength is thus a direct result of the increase in collision energies of the multiple ion–neutral collisions.

The actual peak pressures above the surface after the desorption event can be estimated from the angular measurements described above. A diagram of this estimation (Fig. 4) indicates peak pressures in the region of 1 mbar even at a distance of 100 μm above the surface, a pressure still high enough to induce many ion–molecule collisions.

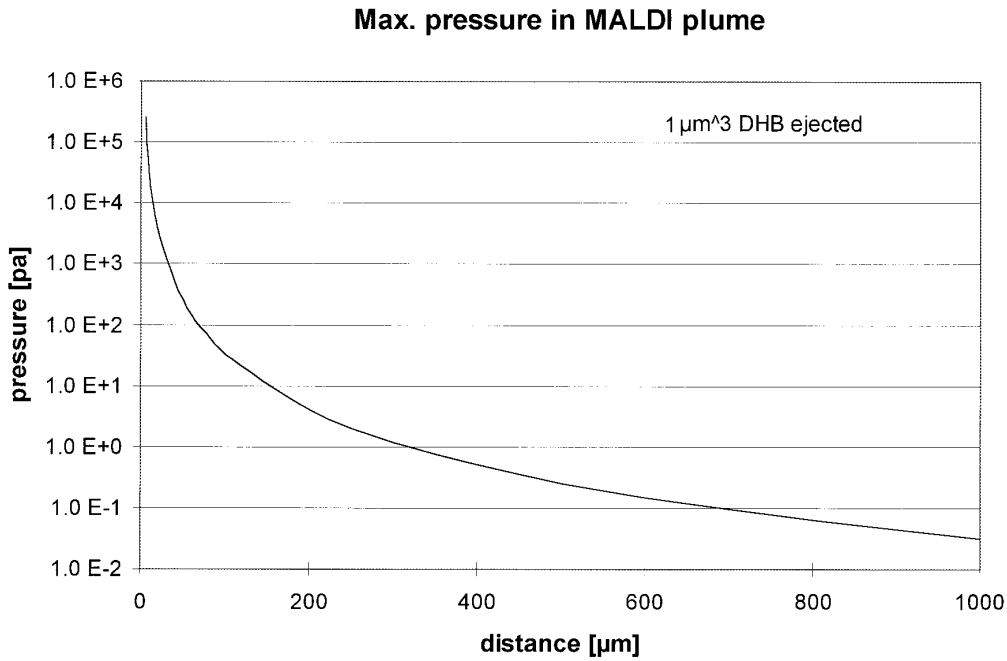

Figure 4. Estimated peak pressures of a MALDI plume derived from experimental data used for Fig. 3.[3] It was assumed that 1 μm^3 of material was ablated by a single laser pulse.

The field-dependent instability of MALDI ions described in Fig. 2 can now be interpreted much more easily. The strong decrease in unimolecular decay with decreasing field strength is simply due to the decrease in the collisional energies of the multiple low-energy collisions in the desorption plume just above the surface during prompt ion acceleration. It is obvious from the data, however, that the unimolecular rate constant does not vanish at zero initial field strength. Another pathway of ion activation seems to exist that is independent of low-energy collisions in the gas phase, taking into account that the slight differences in initial kinetic energies between the ions can be neglected as a source of collisional activation.

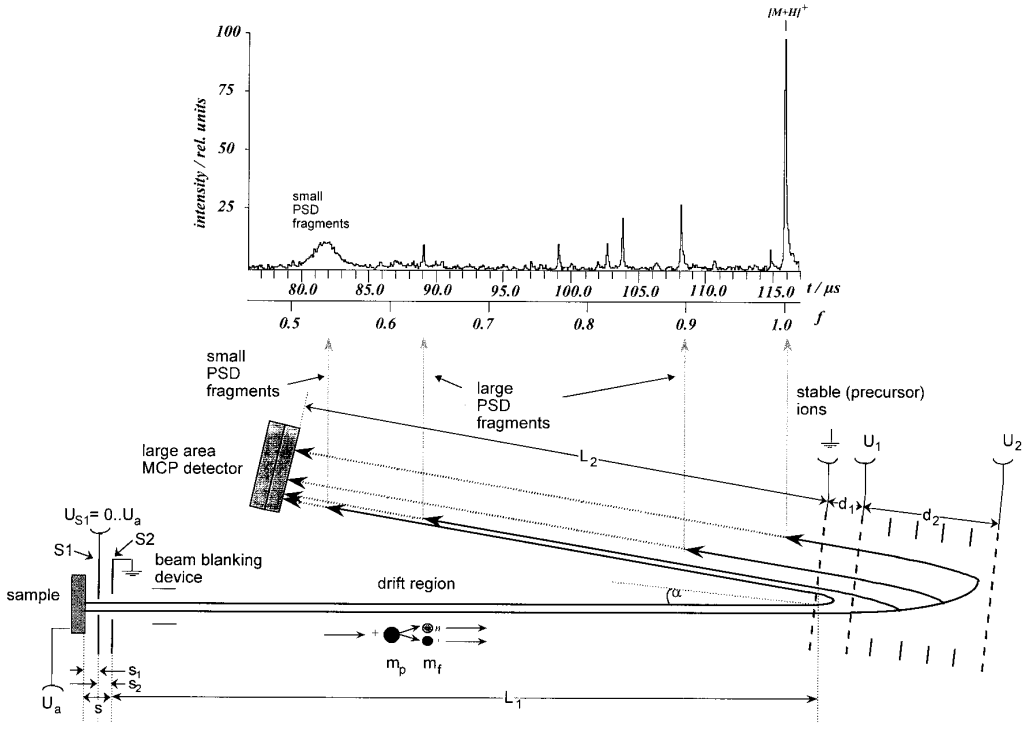

Figure 5. Principle of PSD analysis in MALDI/MS, using a two-stage gridded ion reflector. PSD ions reflected in the second stage of the reflector are imaged as well resolved ion signals in front of the signal of the stable precursor ion signal. Smaller PSD ions reflected in the first stage of the reflector are detected as a broad unresolved signal. Mass analysis of these ions is done in a series of consecutive steps by lowering the potentials U_1 and U_2 of the reflector grids. Total instrument lengths can vary between 1 m and several meters.

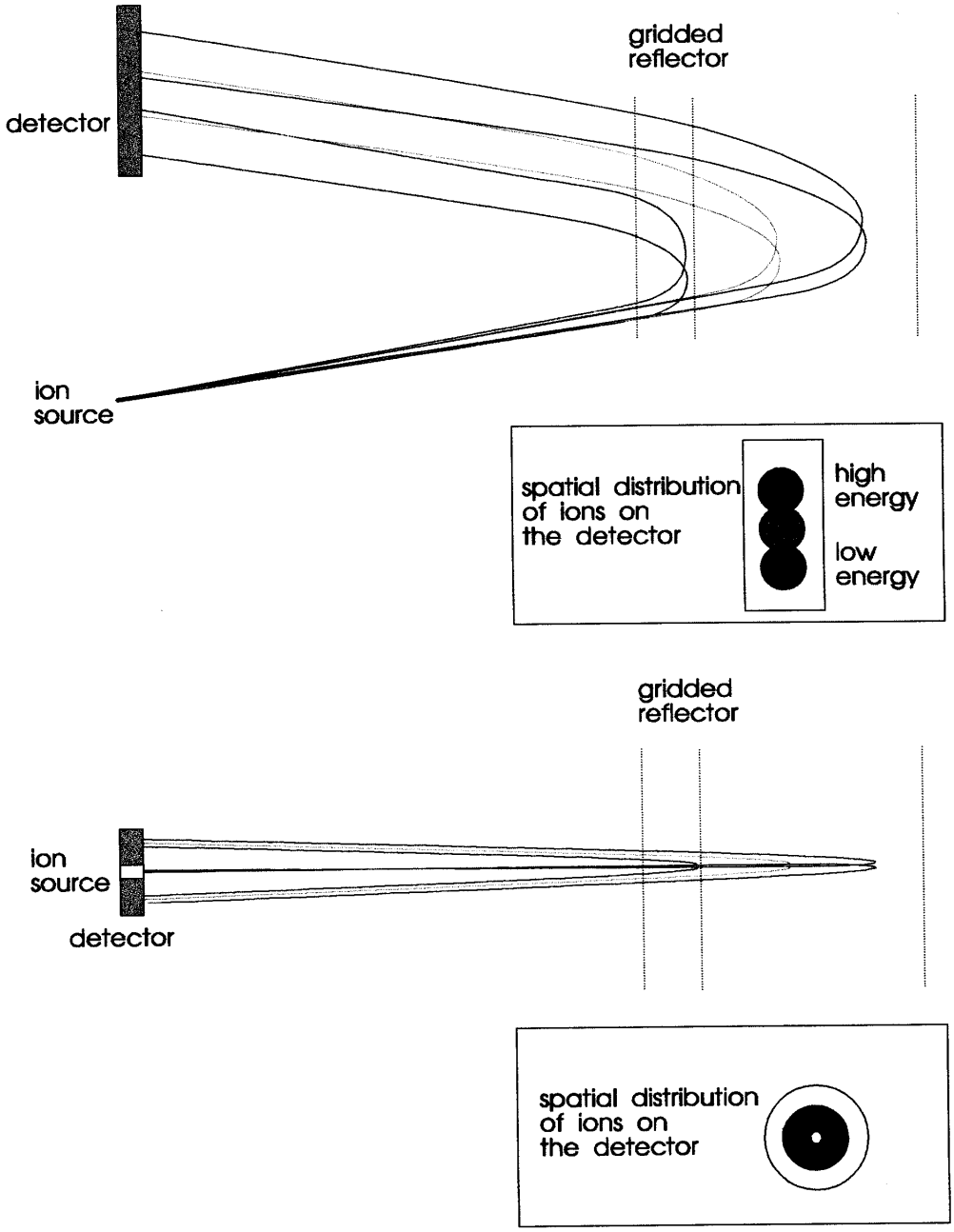

Figure 6. Scheme of PSD reflector geometries. Off-axis instruments (top) require a larger detector and usually a second flight tube. On-axis instruments can be built with one flight tube and with a smaller detector.

Finally, high-energy collisions taking place after ion acceleration in the field-free drift region might play a role in ion activation. They can be controlled (using gas collision cells) or random (due to collisions with residual gas molecules). Table 1 summarizes the three main mechanisms of ion activation in MALDI mass spectrometry.

For PSD analysis all three mechanisms might play an important role. In modern time-of-flight instruments for MALDI-PSD, however, delayed ion extraction is used in order to increase the mass resolution of the observed spectra. In that case, mode 2 of ion activation is of minor importance, since the density of the cloud of neutral molecules is already low at the time of ion acceleration. This, however, does not deteriorate the sensitivity of MALDI-PSD since the lower decay rate is compensated for by the better signal-to-noise ratio due to the increased mass resolving power.[34]

In certain cases, high-energy collisional activation is a favorable activation method for enhancing PSD. The use of the complete instrument as a 'gas collision cell' (by increasing the residual gas pressure) is the easiest way of realizing this appraoch. High-energy collisions taking place at very different locations within the ion beam path, however, lead to measurable peak broadening. Collision cells, on the other hand, have to be designed carefully in order to avoid ion transmission losses.

It has to be kept in mind that for all three activation modes the location of ion decay is always in the field-free drift region, regardless of the location of ion activation.

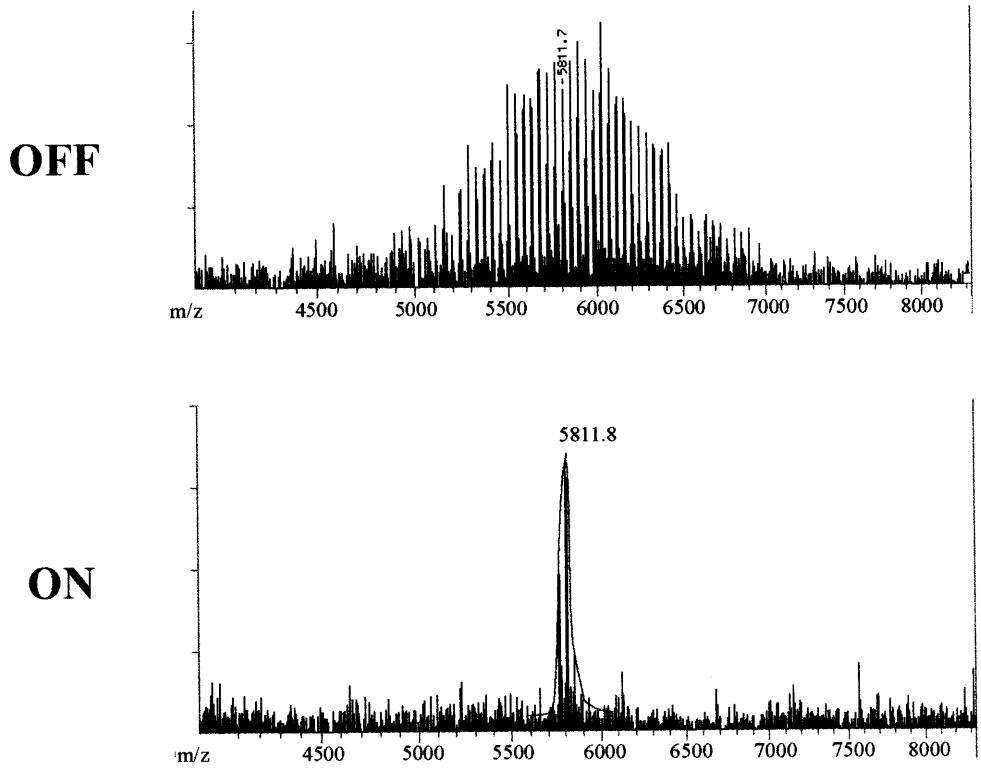

Figure 7. Ion gate performance using a high-voltage switch with a minimum opening time of 80 ns. A gating resolution of 110 is achieved at mass 5811.7 u.

PSD in its physical context is certainly not an exclusive feature of the MALDI source. Mass spectrometric analysis of so-called metastable ions has been known and heavily employed for many years.[35–39] 'Post-source decay' has been chosen as a rather generic *instrumental* term describing the sum of all fragmentation phenomena (metastable ion decay, low-energy collision-induced dissociation, high-energy collision-induced

Table 1 Activation mechanisms in MALDI leading to ion instability and post-source decay

	Mode 1	Mode 2	Mode 3
Activation mechanism	Sample activation	In-source activation	Post-source activation
Activation region	Surface/sample	Selvedge	Vacuum
Activation processes	Direct photon–molecule interactions, solid-state activations, temperature effects, excess energy from ionization	Multiple low to medium energy collisions	High-energy collisions
Time-scale	ps–ns	ns–μs	μs–ms
Distance from surface	0	<200 μm	>acceleration zone

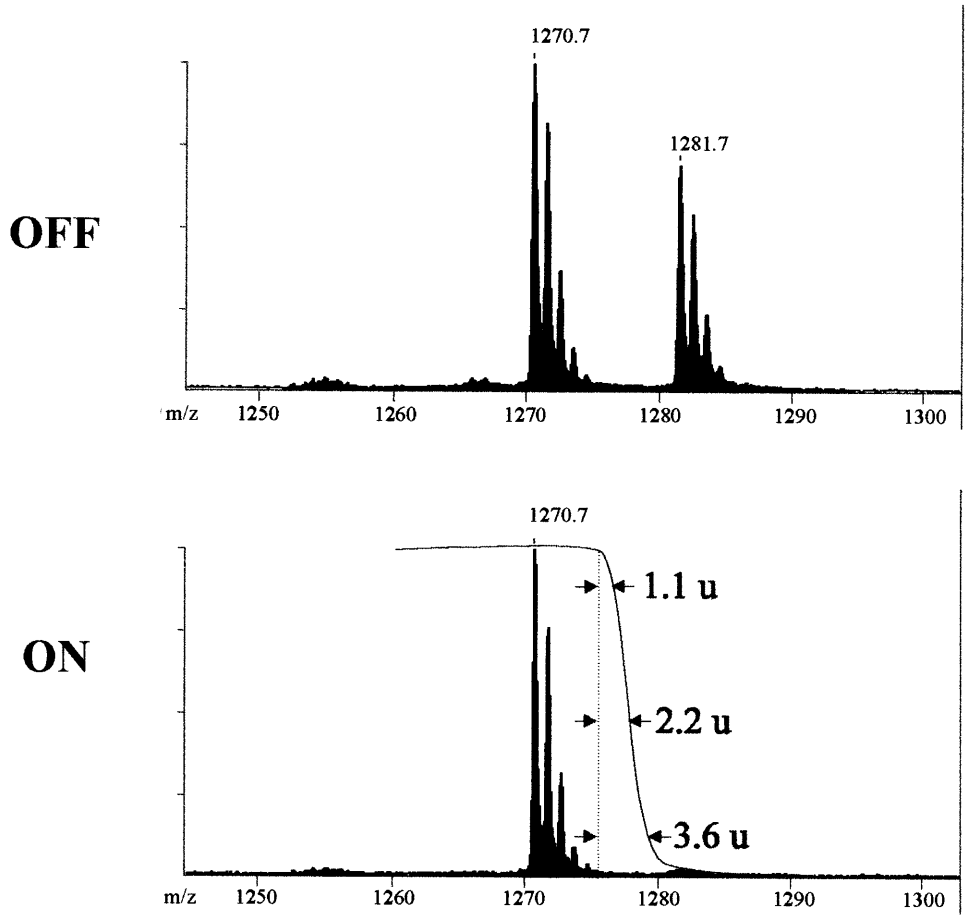

Figure 8. Ion gate performance for cutting an ion beam on one edge only. A selectivity of 512 is achieved for a peptide at mass 1270.6 u.

dissociation as described by activation modes 1–3) relevant for MALDI time-of-flight instruments.

Practical issues of MALDI-PSD analysis

In the PSD mass analysis of biomolecules, the goal is to detect with high sensitivity characteristic product ions, and to interpret with that mass information the primary structure of the precursor molecule. The principle of the set-up of a mass spectrometer for PSD analysis is shown in Fig. 5.

The sample is irradiated by a pulsed UV laser beam of wavelength typically 337 nm (N_2 laser). Ions are formed and accelerated in a two-stage acceleration system, which usually employs pulsed (delayed) ion extraction. After leaving the ion source, all ions have the same nominal kinetic energy, most of them are still unfragmented precursor molecular ions and they have already acquired internal energy by various mechanisms (gas-phase collisions, laser irradiation, thermal mechanisms, etc.). During their flight through the field-free drift region they have a long time available for post-source decay into product ions. These product ions still

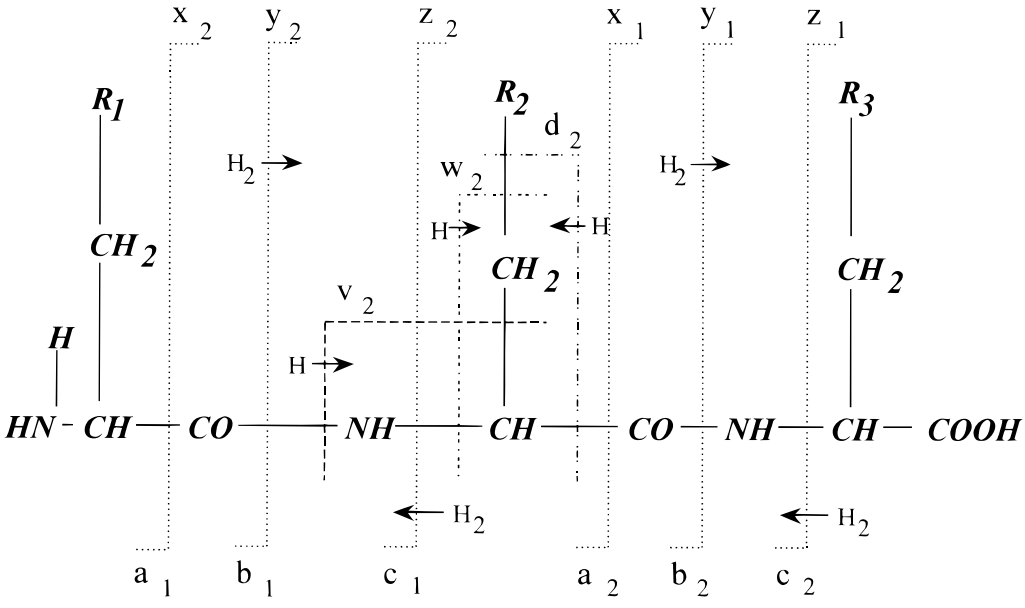

Figure 9. Nomenclature of peptide fragment ions according to Refs 49 and 50.

have basically the same velocity as their precursor ions but now have a much lower kinetic energy owing to their lower mass. The kinetic energy of the product ions is a measure of their mass. In linear instruments, PSD ions are detected at the same time as their precursors and therefore cannot be mass analyzed. The ion reflector, in classical time-of-flight instruments used as a device for flight time compensation of initial energy distributions, is used here as an energy analyzer and thus as a mass analyzer for PSD ions. Owing to their mass-dependent kinetic energies, PSD ions are reflected at different positions within the reflector (at different equipotential surfaces) and thus have mass-dependent total flight times through the instrument.

In typical PSD instruments, a complete product ion spectrum has to be acquired in several steps. This is because an ion reflector as shown in Fig. 5 is able to analyze energies (i.e. PSD ion masses) only within a certain range with sufficient resolution. Part of the product ion spectrum appears as well resolved signals, accompanied by a broad region of lower mass signals. In order to mass analyze these lower mass ions, the potentials of the reflector have to be decreased in steps until all product ions have been imaged with sufficient mass resolution.

Finally, all sections of the PSD spectrum have to be concatenated by the computer and mass calibrated. This method of fragment ion detection is not unique to MALDI-PSD-MS but has been employed earlier in PDMS and SIMS studies of metastable ions.[40,41]

The actual geometry of PSD reflector instruments varies. Off-axis detection[42] (Fig. 6, top) has the advantage of geometrically blanking all secondary ions or electrons formed at the grids of the reflector. As can be seen from the scheme, however, they require a much larger detector, since PSD ions reflected at different positions within the reflector are laterally spread over the detector. Coaxial detection,[43] on the other hand, is possible with a simpler instrumental setup, within the same flight tube and with a smaller detector.

In addition to two-stage gridded reflectors, single-stage reflectors[44] and non-linear reflectors[45] have been used for this kind of analysis as alternative approaches. The non-linear 'curved-field' reflector allows one to acquire PSD spectra in one step without the need for concatenating several spectra but, so far, has not been demonstrated to provide for highest PSD spectral quality with respect to sensitivity, mass resolving power, etc.

Mass calibration of PSD spectra

Mass calibration in PSD analysis is a topic of great importance. In classical time-of-flight analysis of stable ions, mass calibration is fairly easy. Regardless of the number and nature of static acceleration or deceleration fields within the instrument, the mass–time relationship always follows the equation

$$t = a + bm^{1/2} \tag{1}$$

Any time-of-flight spectrum of stable ions can therefore be calibrated by a two-point or least-squares fit calibration using at least two known ion signal masses from calibration substances. Delayed extraction time-of-flight mass spectrometry exhibits some deviation from the strict square-root function which is of practical relevance in linear instruments.[46,47]

In PSD analysis, the situation is much more complicated for two-stage gridded reflectors and for gridless reflectors. There is no analytical function

$$m_{\mathrm{PSD}} = f(t) \tag{2}$$

that could be used for an exact multi-point calibration. Only a rather complicated function

$$t_{\mathrm{PSD}} = f(m_{\mathrm{PSD}}) \tag{3}$$

can be derived, but to use it requires a precise knowledge of all instrumental parameters such as all acceleration and deceleration field strengths and all flight

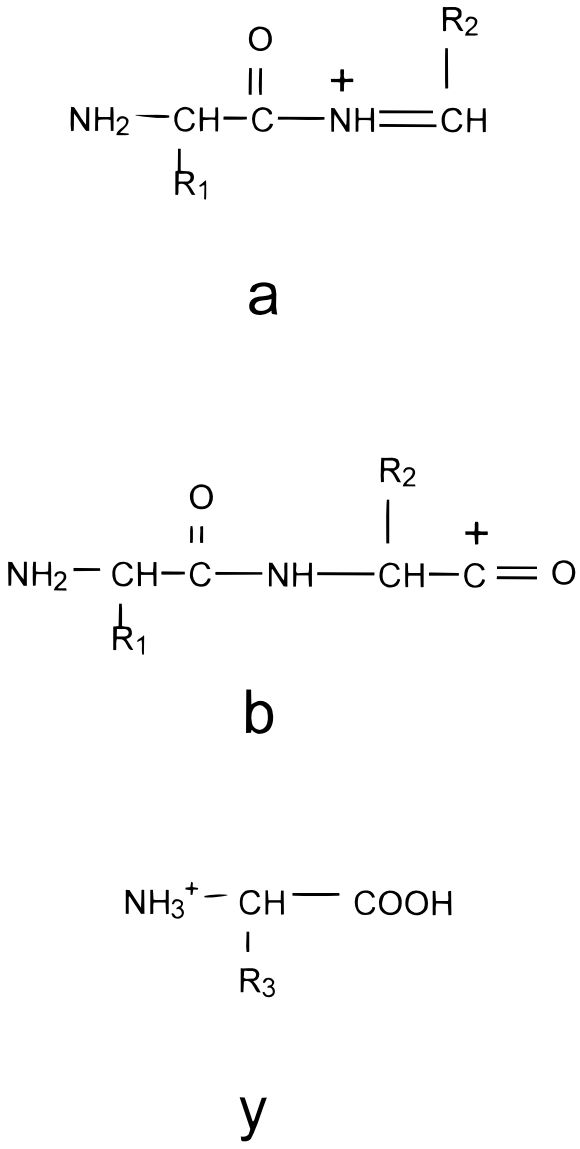

Figure 10. Proposed structures of a-, b- and y-type ions.

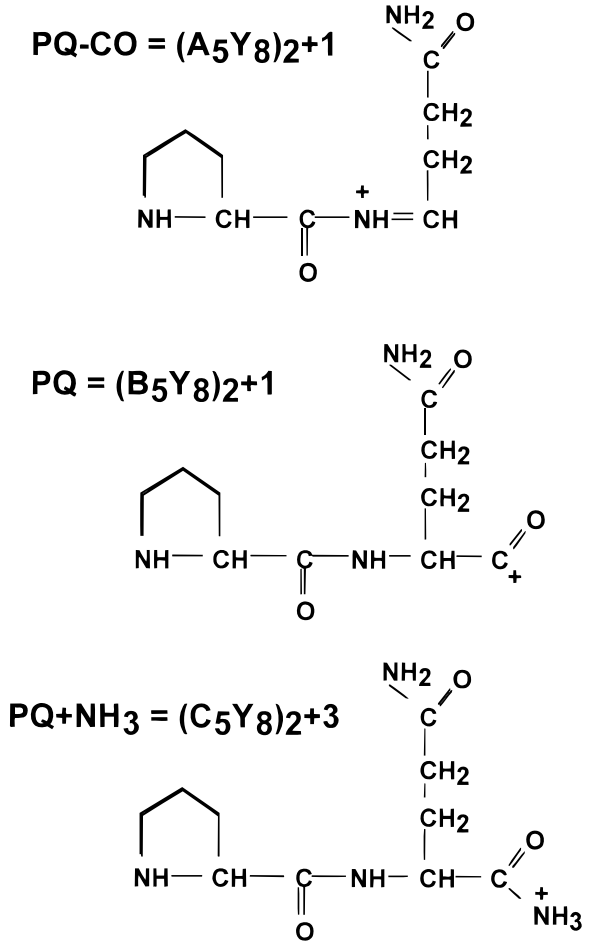

Figure 11. Structure and nomenclature[49,50] of internal ions containing the amino acids P and Q formed from the peptide substance P (RPKPQQFFGLM-NH_2). The nomenclature on the left (PQ, PQ − CO, PQ + NH_3) describes the partial sequence of amino acids contained in the internal ion. The nomenclature on the right (e.g. $(B_5Y_8)_2+1$) describes the internal ion as a product of two regular cleavages, e.g. a B_5 ion which is *N*-terminated by the Y_8 ion structure, which contains two amino acids and which is 1 mass unit higher than the sum of the amino acid masses.

paths. Since usually at least 10–20 parameters are involved, it is much easier to use a different approach which is sufficiently precise for analytical application. This approach uses a polynomial fit with only four parameters:

$$m_{PSD} = a + bt_{PSD} + ct_{PSD}^2 + dt_{PSD}^3 \quad (4)$$

Any flight time curve of any PSD instrument (regardless of the type of reflector used) can be fitted with high accuracy using the third-order polynomial.

To use this method, at least four signals spread over the PSD mass window have to be known in mass and are used for a least-squares polynomial fit.

Precursor ion selection

An important feature of MALDI-PSD instruments is their MS/MS capability, allowing one to preselect a certain precursor ion in a mixture of multiple components, e.g. in a tryptic digestion of a protein. Precursor selection is done by electrostatic 'beam blanking' or 'ion gating.' All ions passing the beam blanking device (Fig. 5) are deflected off the ion detector except a certain mass window which is transmitted without deflection. Deflection is performed by a fast high-voltage drop applied to the device which is typically built of small plates, wires or strips. Positioning of the ion gate within the flight path is always a compromise between position-dependent dispersion of precursor ions of different masses and high transmission for (low-energy) PSD ions already formed at the position of the ion gate. PSD ions are very sensitive to any remaining fringe fields so that the ion gate should be placed at a position where the majority of PSD ions has not yet been formed. The ion gate, on the other hand, has to be located not too close to the source to allow for a sufficient spatial separation of the mass-dependent ion clouds.

Two prerequisites are essential for high-resolution gating. First, the high-voltage switch used has to be fast enough to cut the beam with sufficient resolution. Second, the geometry and field design of the blanking device must lead to a high enough spatial resolution to affect only the ions of interest.

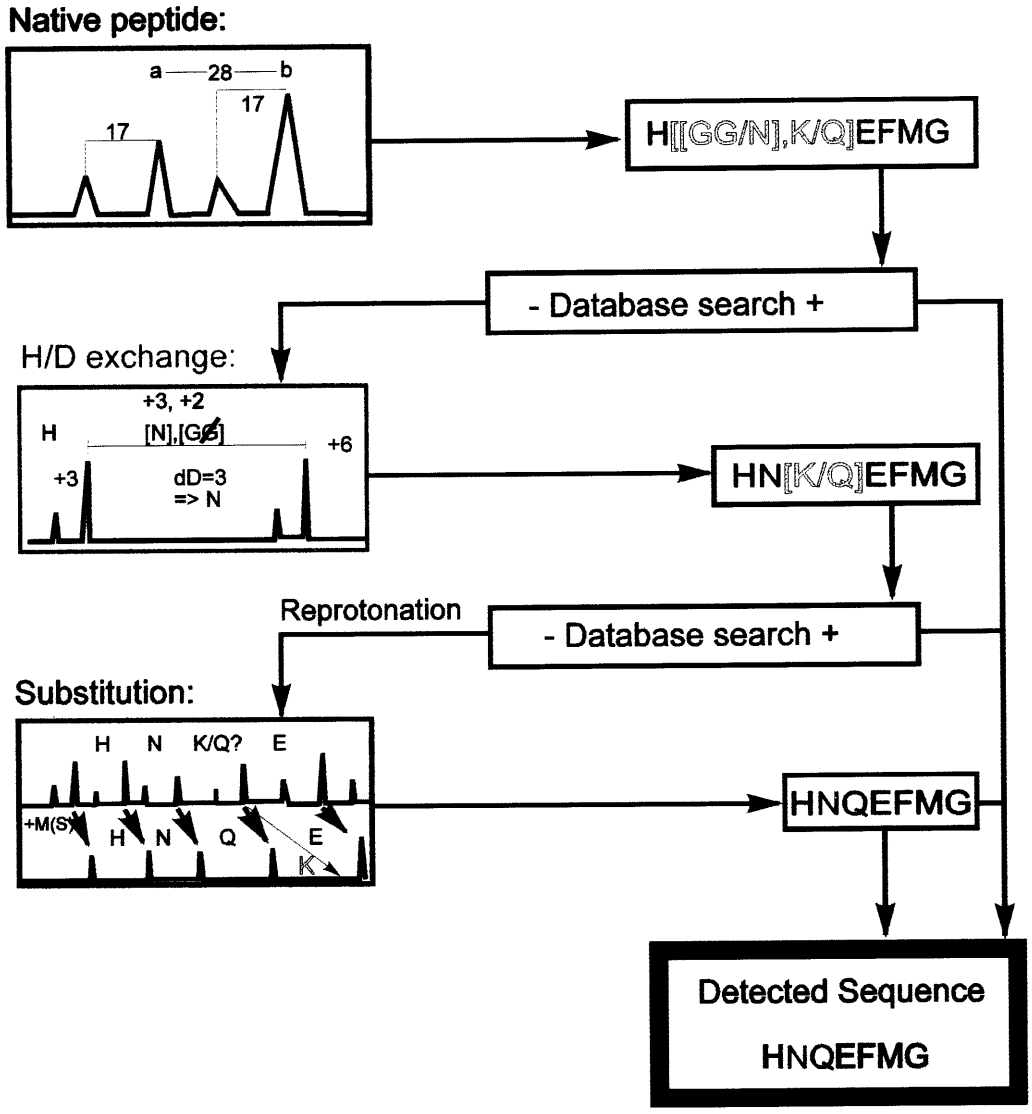

Figure 12. Scheme for a strategy to determine the complete sequence of unknown peptides. Interpretation of product ion spectra of the native peptide sometimes leads to ambiguities. Hydrogen–deuterium exchange, in this example, is able to distinguish between GG and N as the partial sequence, due to the different number of exchangeable hydrogens of the two possibilities. *N*-Terminal acetylation allows the detection of lysine (K) residues since these residues also become acetylated by this derivatization method. In parallel with all steps, database searches can be performed in an attempt to find the sequence in a protein database.

High-voltage switches usually have a limitation in the minimum opening time of the gate. A minimum opening time of 80 ns, for example, limits the selectivity $M/\Delta M$ to values in the range of 110 (FWHM). Figure 7 shows an example of an opening-time limited selectivity for a polyethylene glycol (PEG) 6000. At mass 5811.8 u the neighbouring signals of ± 44 u are decreased in intensity to less than 50% of their original intensity. Newer developments of high-voltage switches will provide for a much shorter minimum opening time and thus a much higher selectivity for cutting both edges of a precursor ion signal.

The actual selectivity of the ion gate itself can be much better demonstrated when cutting the signal from only one edge (Fig. 8). The full width at half-maximum (FWHM) definition, however, is not applicable for describing the selectivity in this case since only one edge is cut. The example in Fig. 8 shows the selection of a peptide at mass 1270.6 u from a mixture with another peptide at mass 1281.6 u. The measurements were performed on an instrument with a first field-free drift length L_1 of 1320 mm, a second drift length L_2 of 970 mm and a distance of the ion gate from the source of 150 mm. As can be seen, the signal at mass 1281.6 u is reduced to much less than 10% of its original intensity whereas the peptide signal at 1270.6 u is not affected in intensity, mass resolution or flight time. It can even be seen that the fifth isotope at mass 1274.6 u is still unaffected by the gating pulse. This means that a mass difference of only 7 u is sufficient to switch the ion beam from 100% to almost zero. The best 'full width at half-maximum' value $M/\Delta M$ that can be expected assuming symmetric selection of the ion gate is 580/2. A more realistic description is to use the 'rise mass' (analogous to the rise time definition in electronic engineering) for a drop from 90% down to 10%. For the example shown here, a rise mass of 2.5 u is found, corresponding to a selectivity $M/\Delta M$ of 512. From the practical point of

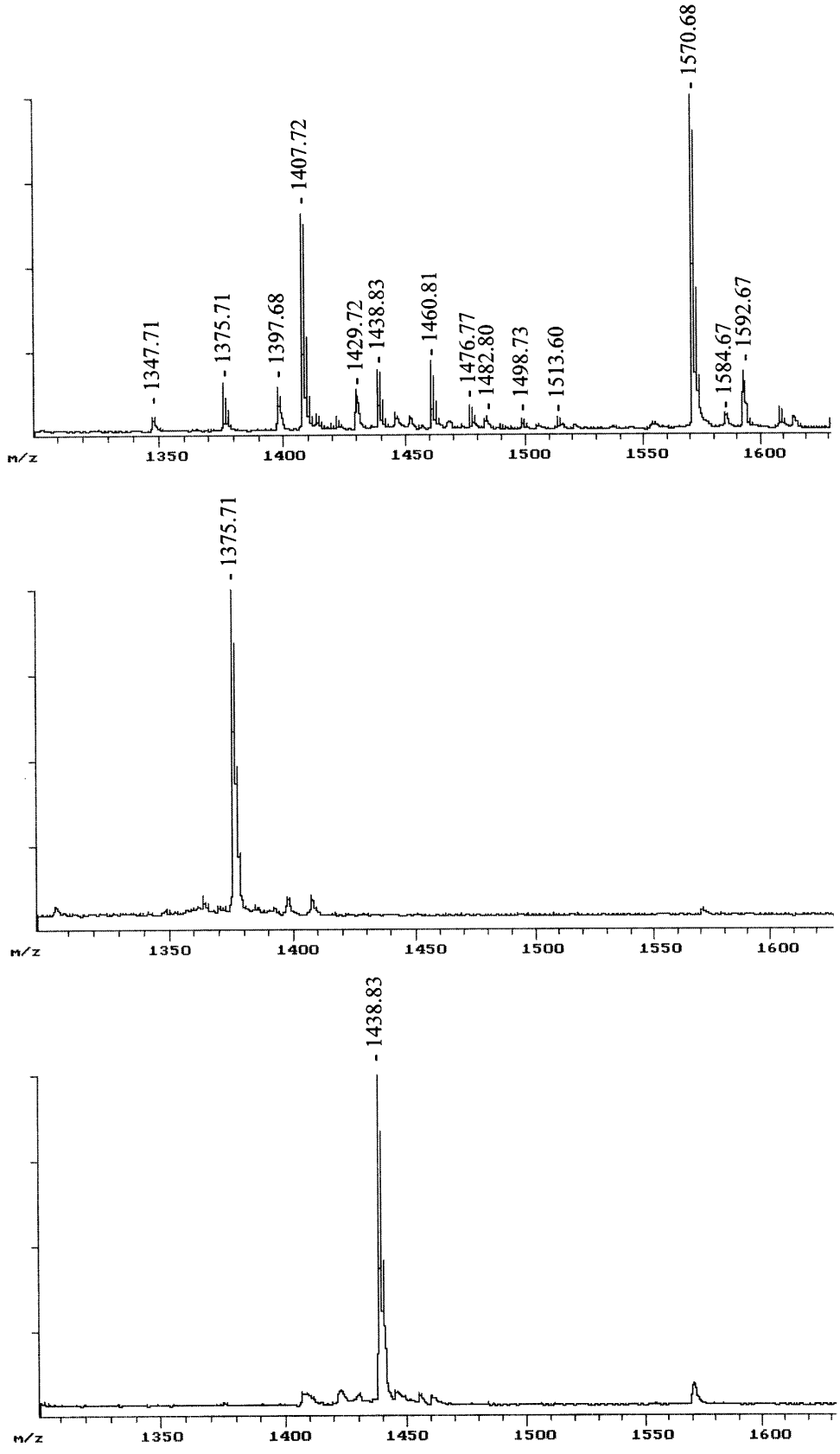

Figure 13. MALDI mass spectrum of a contest sample containing 10 different peptides. Upper spectrum: ion gate off. Middle spectrum: ion gate on and set to transmit the peptide at 1375.8 u. Lower spectrum: ion gate on and set to transmit the peptide at 1438.7 u. Spectra acquired on ALADIM I, Institute of Laser Medicine, Düsseldorf.

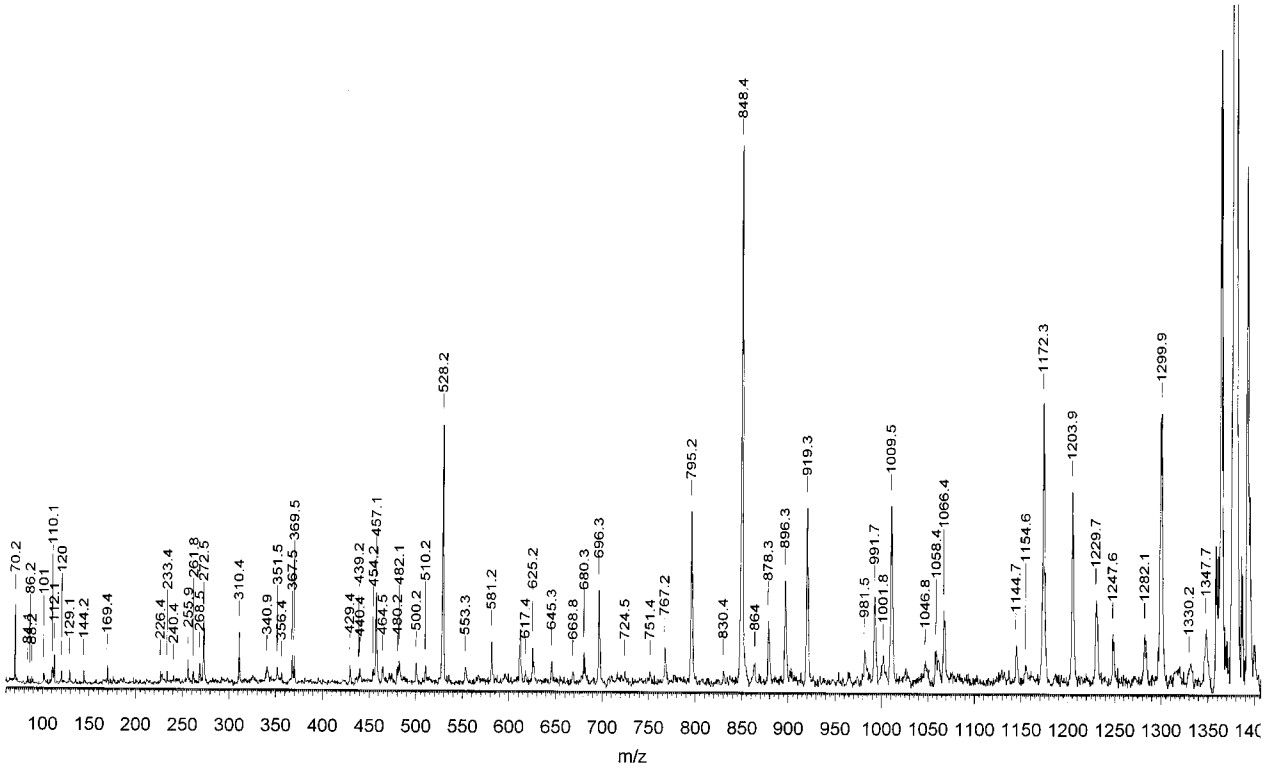

Figure 14. MALDI-PSD mass spectrum of peptide at $[M + H]^+ = 1375.8$ u acquired on ALADIM I, Institute of Laser Medicine, Düsseldorf.

view this means that PSD analysis can be performed on mixtures of peptides that differ in mass by only a very few mass units.

APPLICATIONS AND INTERPRETATION OF SPECTRA

The majority of applications employing MALDI-PSD/MS have concentrated on peptide characterization and peptide sequencing so far, rather than on the analysis of other biomolecules, mainly driven by the analytical demand rather than by methodological limitations. For peptides the sensitivity of the method is in the range 30–100 fmol prepared sample. Using delayed ion extrac-

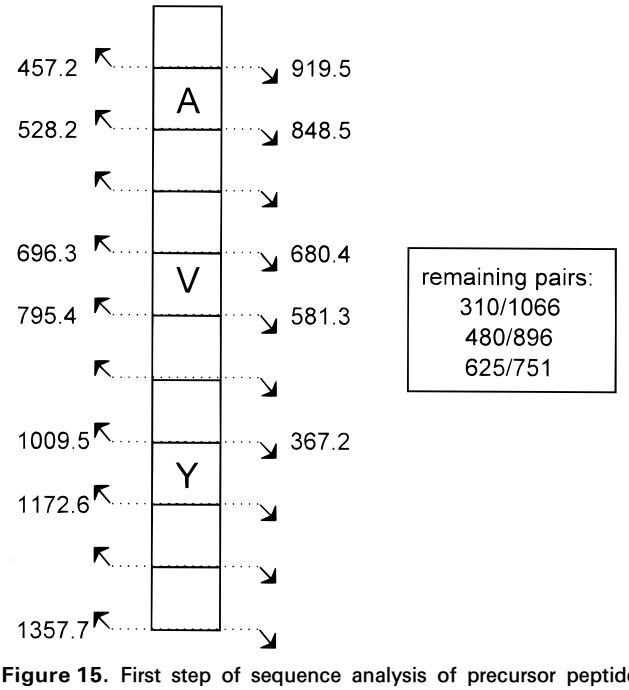

Figure 15. First step of sequence analysis of precursor peptide ion at 1375.8 u. *N*-Terminal end on top. Indicated are observed b-type (left) and y-type (right) ions only.

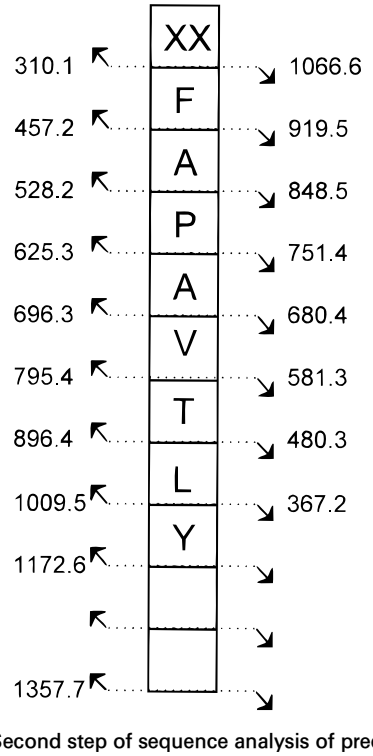

Figure 16. Second step of sequence analysis of precursor peptide ion at 1375.8 u. *N*-Terminal end on top. Indicated are observed b-type (left) and y-type (right) ions only.

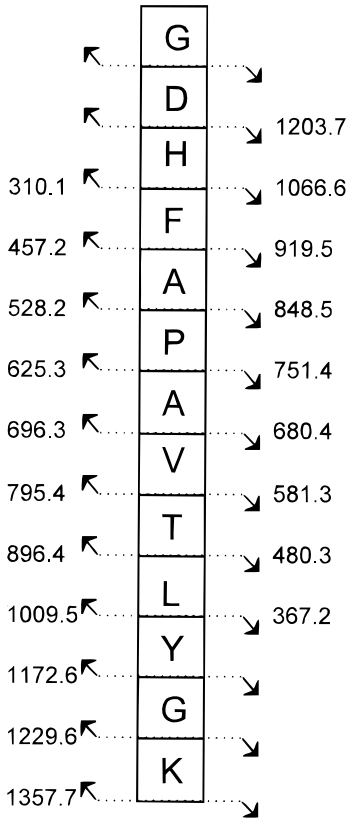

Figure 17. Final sequence determined for precursor peptide ion at 1375.8 u. *N*-Terminal, end on top. Indicated are observed b-type (left) and y-type (right) ions only. 'K' in the scheme is either K (lysine) or Q (glutamine), 'L' is either L (leucine) or I (isoleucine).

tion, the mass resolving power for precursor ions is in the range 6000–10 000, whereas for PSD ions it is in the range 1500–2000. The accuracy of mass determination strongly depends on the calibration method used (i.e. internal or external) and can be as high as ± 10 ppm.

The high senstivity of MALDI-PSD is produced by the long time available for ion decay between leaving the ion source and entering the ion reflector. This time can be in the range 50–100 μs. Owing to the long time frame, the resulting fragment ion pattern is more thermodynamically controlled rather than kinetically controlled. Faster decay reactions are detected with a probability similar to slower decay reactions. Another important and characteristic side-effect of this behavior is that not only single-step but also multiple-step fragmentations are observed. Internal ions, which contain neither end of the molecule chain, are the result of at least two cleavage reactions. The prerequisite for multiple fragmentation reactions to be detected in PSD spectra is not so much the reaction rate constants but more the internal energy required for the reactions to take place. An example of up to four consecutive cleavage reactions observed as internal ion signals in a PSD spectrum was demonstrated for a branched triantennary oligosaccharide[48] that showed internal ions of the inner core with abundances comparable to those of the terminal fragment ions.

For peptides, the formation of internal ions is also pronounced. Figure 9 describes the nomenclature for *C*- and *N*-terminal ions of peptides. Not all of these ion types are actually observed with high abundances. The most common PSD fragment ion types are a, b, y, z and d ions. All of these ion types can be accompanied by satellites due to loss of ammonia (-17 u) or water (-18 u). The proposed structures of a-, b- and y-type ions are shown in Fig. 10.

The formation of internal ions exhibits a characteristic sequence specificity. Most pronounced are internal ions extending in the *C*-terminal direction from a proline. This 'proline-directed internal fragmentation' contains valuable analytical information for the confirmation of a proposed amino acid sequence, since peptides containing proline never fail to form a series of proline-directed internal fragments. The structure and nomenclature of internal fragments are summarized in Fig. 11. Only those three types of internal fragment ions have been observed, accompanied again by satellites due to loss of ammonia or water.

Immonium ions of the amino acids present in the peptide are another analytically important class of internal ions. A considerable fraction of the amino acids form these characteristic low-mass ions and can thus be confirmed or rejected as being present in the unknown peptide.

Strategies for sequencing unknown peptides

Owing to the complexity of possible fragmentation patterns and to ambiguities in mass signal interpretation, peptide sequencing of completely unknown peptides is not always a straightforward task. Additional techniques that provide more structural information are sometimes required to determine a peptide sequence unequivocally. The scheme in Fig. 12 describes a strategy for unknown peptides using additional tools such as hydrogen–deuterium exchange and *N*-terminal acetylation.

A number of possible derivatization methods are known that help to solve special problems of sequence ambiguities, including *N*-terminal charge derivatization[51–53] and arginine blocking.[52] Hydrogen–deuterium exchange, however, has been found to be the most general and easiest approach for obtaining additional structural information in mass spectrometric peptide sequencing.[54] Information on the total number of exchangeable hydrogens of both the precursor ion and the characteristic product ions decreases the number of possible interpretations by orders of magnitude in general. The method can be performed with femtomolar amounts of sample on target within a few minutes.

Sequencing of an unknown peptide

As an example an sequencing an unknown peptide, a sample has been chosen from the instrumental contest performed at the annual conference 'Mikromethoden in der Proteinchemie' held at the Max-Planck-Institut für Biochemie, Martinsried, Germany, June 22–26, 1997. The sample '2' given to all participants in the contest contained a mixture of 10 peptides accompanied by derivatives of these peptides. Two of these peptides at mass 1375.8 u and 1357.7 u had to be analyzed in order to determine their amino acid sequence. Figure 13 shows the MALDI mass spectrum of the mixture without and with ion gating of the two species.

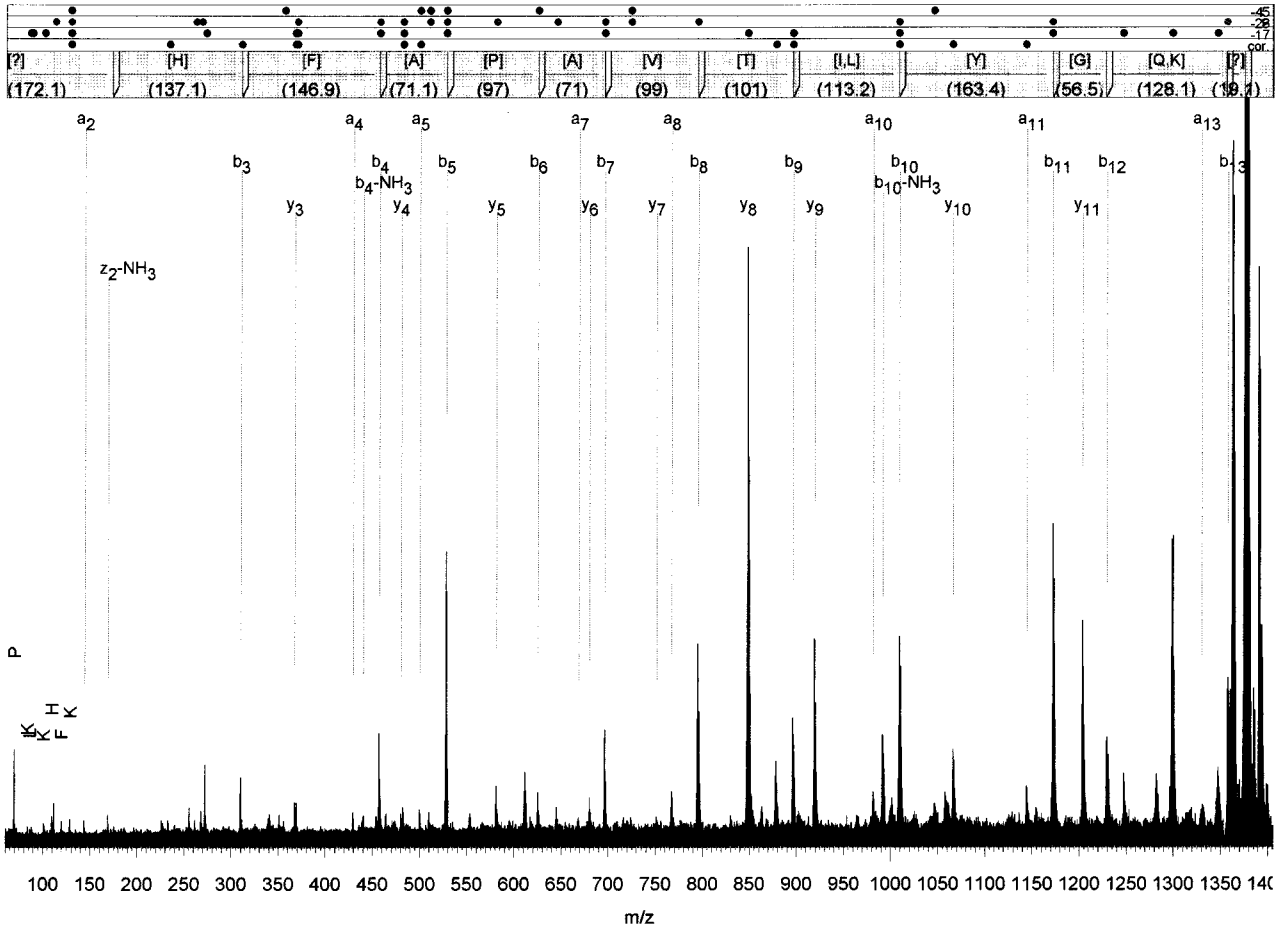

Figure 18. MALDI-PSD mass spectrum of the peptide at $[M + H]^+ = 1375.8$ u acquired on ALADIM I, Institute of Laser Medicine, Düsseldorf. Labeled are the ion signals interpreted as *N*-terminal and *C*-terminal ions. The bar above the labels describes the amino acid sequence determined. Dots in the top part of the figure correspond to neighborhood analysis of peaks (presence of a-type neighbors to b-type ions, satellites, etc.).

PSD analysis of the peptide at mass 1375.8 u is described in the following. The PSD spectrum is shown in Fig. 14. The low-mass end of the spectrum indicates the presence of the amino acids P (70 u), K/Q (84, 101, 112, 129 u), I/L (86 u), [D (88 u)], H (110 u) and F (120 u) and the absence of W (159 u). The absence or presence of the other amino acids cannot be decided from the data. Correspondences between *N*- and *C*-terminal ions according to the relationship

$$m_b + m_y = m_{precursor} + 1$$

(m_b, m_y and $m_{precursor}$ being the masses of the b- and y-type fragment and precursor ions, respectively) were found for the mass signal pairs 310/1066, 367/1009, 457/919, 480/896, 528/848, 581/795, 625/751 and 680/696 u. It can be assumed that one of each pair is a b-type ion and the other is a y-type ion. Neighboring signals resulting from a-type ions or a- or b-type satellites indicating 'b' as the correct fragment ion type were found for 457, 528, 696, 795, 1009, 1172 and 1357 u. With that information, three positions within the peptide chain could already be interpreted. Figure 15 describes the sequence information that is already confirmed by the data.

The gap between 528 and 696 u can only be occupied by the doublet PA (or AP) or GU (or UG). Assuming that the corresponding b-type ion is contained in the list of remaining ion pairs, only PA appears to be a probable partial sequence.

In analogy, the gap between 795 and 1009 u can be occupied by the doublets UC, DV or LT. Only TL is verified by the appearance of a b/y ion pair.

The remaining ion pair 310/1066 u finally only fits the *N*-terminal end of the confirmed partial sequence, corresponding to a phenylalanine. The sequence proposed so far is shown in Fig. 16.

The *C*-terminal gap between 1172.6 and 1357 u can be filled by the doublets NA or (K/Q)G. Only the partial sequence G(K/Q) is supported by a PSD ion signal at 1229.6 u.

Taking into account the information on present or absent amino acids from immonium ions, the remaining partial sequence at the *N*-terminus can only be filled by the partial sequence GDH (or permutations of it). Since the immonium ion signal from aspartic acid (D) is not a very reliable constraint, the partial sequence ATH (or permutations) has to be taken into account as another possibility. Since cleavages of ions extending in the *C*-terminal direction from an aspartic acid (D) are known to be fairly prominent, one can expect to see this cleavage as an intense signal in the PSD spectrum. The only partial sequence matching the observed PSD ion signals is GDH, supported by the ion signal at 1203.7 u. The other possible sequences DGH, ATH or TAH are less

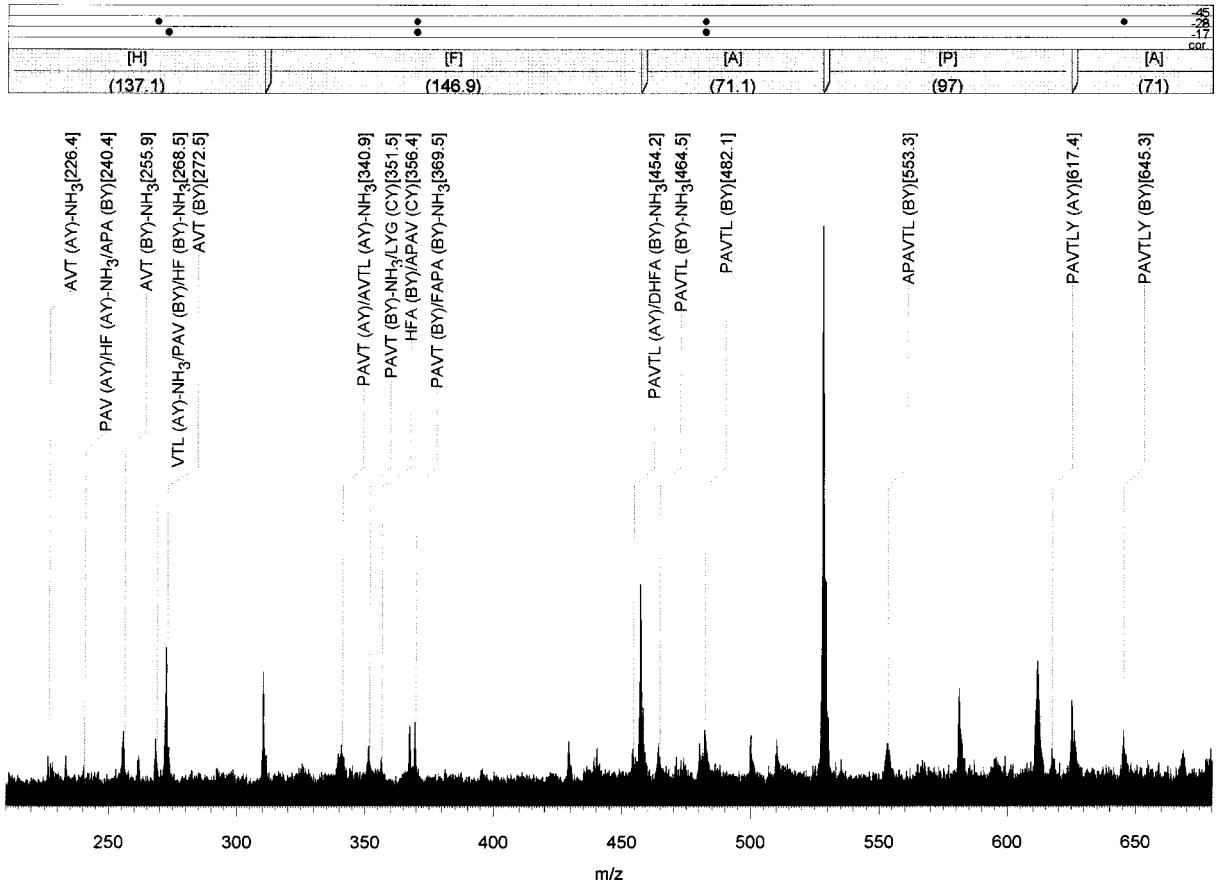

Figure 19. Lower mass part of the MALDI-PSD mass spectrum of peptide at $[M + H]^+ = 1375.8$ u. Labeled are the ion signals interpreted as internal ions. The bar above the labels describes the amino acid sequence determined. Dots in the top part of the figure correspond to neighborhood analysis of peaks (presence of a-type neighbors to b-type ions, satellites, etc.).

likely because of the aspartic acid constraint as mentioned. The final (and correct) sequence proposed from the native PSD spectrum is shown in Fig. 17.

Confirmation of the proposition is made by comparison of the expected fragmentation pattern with the actual spectrum. Unexplained prominent peaks in the PSD spectrum are always a strong hint for certain misinterpretations. Figure 18 shows the observed spectrum again, labeled with the expected *C*- and *N*-terminal fragment ion descriptions.

The matching between expected and observed internal ions is another strong indication of the correctness of a proposition. Figure 19 shows the lower mass part of the spectrum, now labeled with the descriptions of internal ions.

Finally, a confirmation by hydrogen–deuterium exchange is suggested, since a few uncertainties in the sequence proposition remained at the termini of the peptide. The observed mass of the deuterated precursor ion of 1396.9 u, and the observed mass signals of the PSD ions, strongly support the sequence proposition in Fig. 17.

The lysine residue proposed in Fig. 17 could also be a glutamine and leucine could also be an isoleucine. As mentioned earlier, lysine and glutamine can be differentiated by an acetylation experiment.

After having reached a high degree of certainty for a proposed amino acid sequence of an unknown peptide, the most convincing confirmation is to synthesize the peptide and compare the PSD spectra of the native peptide and the synthetic peptide. Correct propositions are usually characterized by a very high similarity of the two spectra, both in signal intensities and signal presence, even if the homogeneity and purity of the two samples and the instrumental or preparation conditions are different.

Database-assisted sequencing of peptides

The other peptide in the contest sample at 1438.8 u is an example where the complete sequence of the peptide can be found by a protein database search after determination of just a partial sequence and amino acid information by PSD spectral interpretation. In addition to database searching of uninterpreted data,[8,55] this 'sequence tag approach'[56] has been found to be a very powerful method for peptides derived from database-listed proteins. Figure 20 shows the PSD spectrum of the gated signal of the 1438.8 u precursor. *C*- and *N*-terminal ion correspondences have been found for the pairs 227.1/1212.9, 355.2/1084.8, 390.1/1049.9, 452.1/987.9, 503.5/936.8, 565.0/874.0, 631.1/808.7 and 693.3/747.3 u.

The ion signal at 1049.9 u could be interpreted as a b-ion from the observation of a corresponding a-ion and [a − 17] satellite ion. Starting with this signal, the next b ion in the *N*-terminal direction can only be 936.8 u from the list of corresponding ion pairs, according to a leucine or isoleucine. The next b ion can be assumed

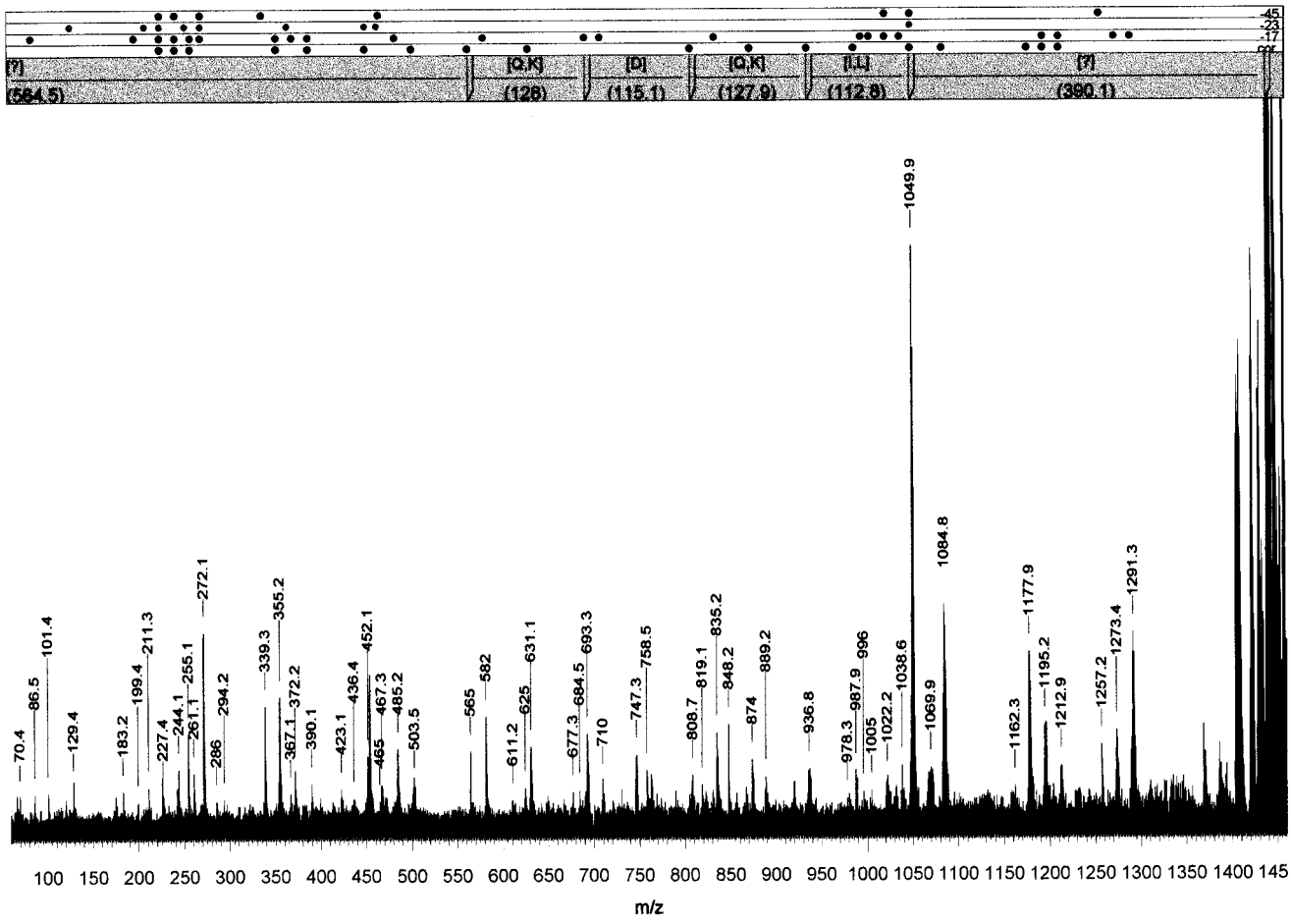

Figure 20. MALDI-PSD mass spectrum of the peptide $[M + H]^+ = 1438.8$ u acquired on ALADIM I, Institute of Laser Medicine, Düsseldorf. The bar above the labels describes a partial amino acid sequence determined for performing a protein database search. Dots in the top part of the figure correspond to neighborhood analysis of peaks (presence of a-type neighbors to b-type ions, satellites, etc.).

to be at mass 808.7 u, corresponding to a lysine or glutamine or to an alanine–glycine doublet. Aspartic acid and another K/Q or AG follows. This sequence information should be sufficient to form a reasonable sequence tag of the form (565.0)KDKL(1049.9). In the search, K should be permuted with Q, AG and GA. Only two sequence propositions result from a database search using this tag, LIQPIQDKIKNE derived from phosphoenolpyruvate protein phosphotransferase PT1_STAAU and NEFSSQDQLNQE from a gene product 'C06A6.5'. By comparison of the expected fragmentation patterns of the two propositions with the observed spectrum, it is immediately confirmed that LIQPIQDKIKNE is the correct sequence. Figure 21 lists the pattern of expected and observed fragment ion masses of the peptide.

Primary structure analysis of other biomolecules

Primary structure analysis of peptides is obviously the main target so far for mass spectrometric sequencing techniques. PSD analysis of other biomolecules such as oligonucleotides,[7] oligosaccharides,[48,57–59] branched peptides,[12,60] conjugates,[6] etc., however, is possible with the same level of quality, information content and reliability, but interpretation strategies for these compounds still have to be developed individually.

CONCLUSION

Post-source decay analysis of ions formed by MALDI has become a valuable MS/MS technique for the structure analysis of biomolecules. Owing to the well established features of MALDI for handling small quantities of complex or minimally purified samples, PSD analysis in many cases has some advantages over other MS/MS techniques such as electrospray/triple quadrupole mass spectrometry. Owing to the solid-phase nature of the MALDI technique, on-line coupling to separation techniques and large-scale automation of PSD analysis, however, is much more complicated than in the case of electrospray ionization. MALDI-PSD therefore has to be considered so far as a valuable complementary method rather than a substitute for other ionization techniques.

One of the most challenging applications of mass spectrometry is in the analysis of MHC restricted peptide pools presented on the surface of vertebrate cells, owing to the extreme heterogeneity of samples even after affinity chromatography and reversed-phase

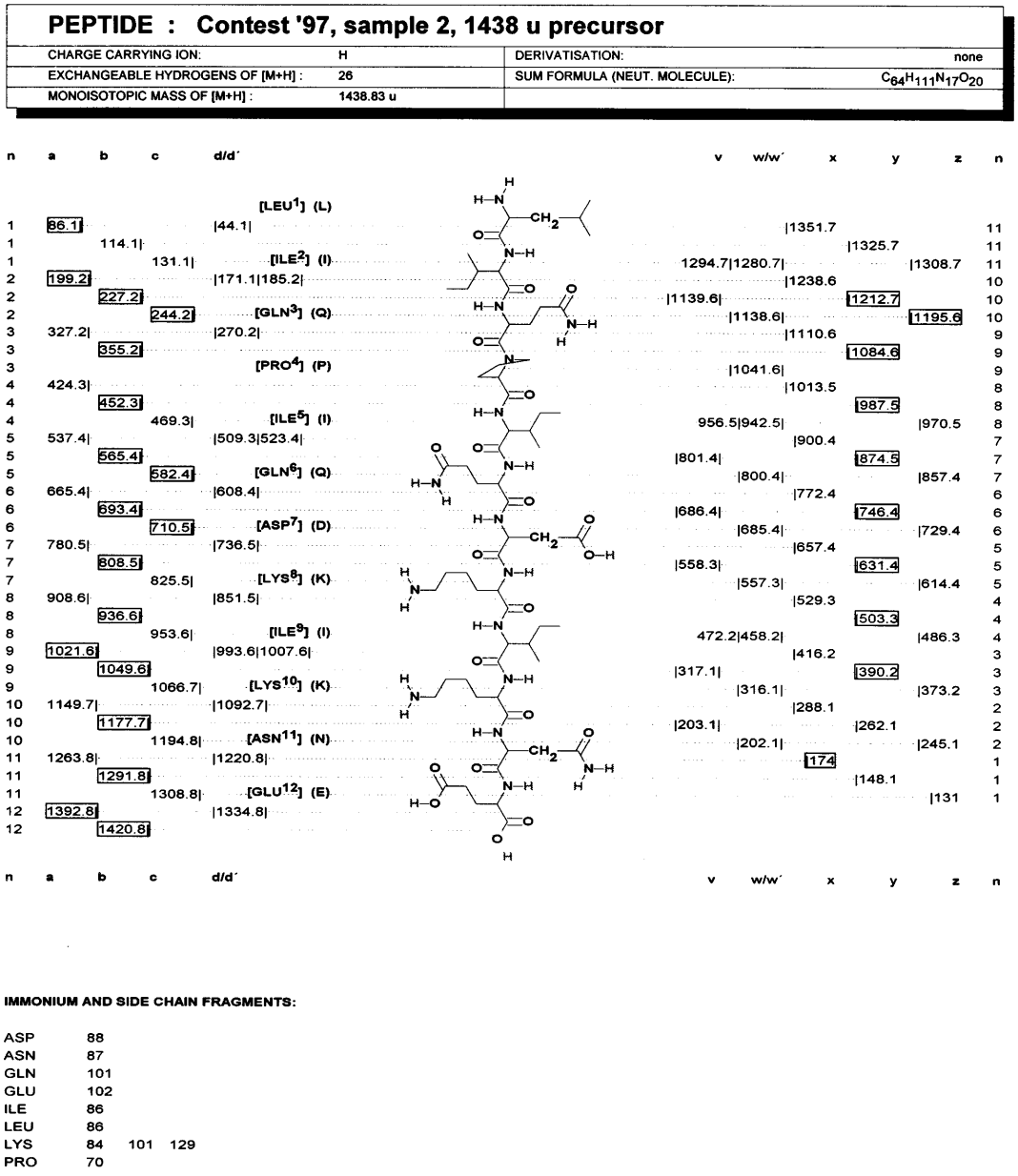

Figure 21. Fragmentation scheme of the peptide LIQPIQDKIKNE ($[M + H]^+ = 1438.8$ u). Masses of ion signals observed in the spectrum are marked.

high-performance liquid chromatographic fractionation, and owing to the small quantities of material available, which is typically in the region of 100 fmol per peptide. In addition to electrospray ionization,[61] MALDI-PSD has now been shown to provide a promising strategy for the detection and characterization of immunologically relevant peptides.[62]

The routine applicability of MALDI-PSD is now mainly a question of automation and software-assisted spectra interpretation. There is no doubt that within a short period MALDI-PSD will be established as a fully developed routine technique for the automated large-scale sequencing of peptides and other biomolecules.

Acknowledgements

Financial support by the Bundesministerium für Bildung, Wissenschaft, Forschung und Technologie (BMBF) (contract No. 0310709), by the European Community (contract No. MAT1-CT94-0034), by the Ministerium für Wissenschaft und Forschung, Nordrhein-Westfalen, and by Thermo Bioanalysis Ltd, Hemel Hempstead, UK, is gratefully acknowledged.

REFERENCES

1. R. Kaufmann, B. Spengler and F. Lützenkirchen, *Rapid Commun. Mass Spectrom.* **7**, 902 (1993).
2. R. Kaufmann, D. Kirsch and B. Spengler, *Int. J. Mass Spectrom. Ion Processes*, **131**, 355 (1994).
3. B. Spengler, D. Kirsch and R. Kaufmann, *J. Phys. Chem.* **96**, 9678 (1992).
4. B. Spengler, D. Kirsch, R. Kaufmann and E. Jaeger, *Rapid Commun. Mass Spectrom.* **6**, 105 (1992).
5. W. Yu, J. E. Vath, M. C. Huberty and S. A. Martin, *Anal. Chem.* **65**, 3015 (1993).

6. M. C. Huberty, J. E. Vath, W. Yu and S. A. Martin, *Anal. Chem.* **65**, 2791 (1993).
7. W. G. Critchley, J. B. Hoyes, A. E. Malsey, M. A. Wolter, J. W. Engels and J. Muth, in *Proceedings of the 42nd Annual Conference on Mass Spectrometry and Allied Topics*, Chicago, IL, May 29–June 3, 1994.
8. R. R. Griffin, M. J. MacCoss, J. K. Eng, R. A. Blevins, J. S. Aaronson, J. R. Yates, III, *Rapid Commun. Mass Spectrom.* **9**, 1546 (1995).
9. J. Stahl-Zeng, F. Hillenkamp and M. Karas, *Eur. Mass Spectrom.* **2**, 23 (1996).
10. K. F. Medzihradszky, G. W. Adams, A. L. Burlingame, R. H. Bateman and M. R. Green, *J. Am. Soc. Mass Spectrom.* **7**, 1 (1996).
11. T. J. Cornish and R. J. Cotter, *Rapid Commun. Mass Spectrom.* **8**, 781 (1994).
12. R. Kaufmann, D. Kirsch, J. L. Tourmann, J. Machold and F. Hucho, *Eur. Mass Spectrom.* **1**, 313 (1995).
13. K. Biemann and S. A. Martin, *Mass Spectrom. Rev.* **6**, 1 (1987).
14. K. Biemann, *Annu. Rev. Biochem.* **61**, 977 (1992).
15. M. Wilm, A. Shevchenko, T. Houthaeve, S. Breit, L. Schweigerer, T. Fotsis and M. Mann, *Nature* (*London*) **379**, 466 (1996).
16. M. Moormann, U. Zahringer, H. Moll, R. Kaufmann, R. Schmid and K. Altendorf, *J. Biol. Chem.* **272**, 10729 (1997).
17. C. L. Nilsson, C. M. Murphy and R. Ekman, *Rapid Commun. Mass Spectrom.* **11**, 610 (1997).
18. T. Yamagaki, Y. Ishizuka, S.-I. Kawabata and H. Nakanishi, *Rapid Commun. Mass Spectrom.* **11**, 527 (1997).
19. H. Schlueter, D. Mentrup, I. Gross, H. E. Meyer, B. Spengler, R. Kaufmann and W. Zidek, *Anal. Biochem.* **246**, 15 (1997).
20. D. Veelaert, B. Devreese, L. Schoofs, J. Van Beeumen, J. Vanden Broeck, S. S. Tobe and A. De Loof, *Mol. cell. Endocrinol.* **122**, 183 (1996).
21. M. Wilm, T. Houthaeve, G. Talbo, R. Kellner, P. Mortensen and M. Mann, in *Mass Spectrometry in Biological Science*, edited by A. Burlingame and S. A. Carr, pp. 245–265. Humana Press, Totowa, NJ (1996).
22. D. J. Harvey, *J. Chromatogr. A* **720**, 429 (1996).
23. J. Machold, Y. Utkin, D. Kirsch, R. Kaufmann, V. Tsetlin and F. Hucho, *Proc. Natl. Acad. Sci. USA* **92**, 7282 (1995).
24. M. Karas, D. Bachmann, U. Bahr and F. Hillenkamp, *Int. J. Mass Spectrom. Ion Processes* **78**, 53 (1987).
25. M. Karas and F. Hillenkamp, *Anal. Chem.* **60**, 2299 (1988).
26. F. Hillenkamp, M. Karas, R. C. Beavis and B. T. Chait, *Anal. Chem.* **63**, 1193A (1991).
27. B. Spengler, D. Kirsch, R. Kaufmann, M. Karas, F. Hillenkamp and U. Giessmann, *Rapid Commun. Mass Spectrom.* **4**, 301 (1990).
28. B. Spengler and R. J. Cotter, *Anal. Chem.* **62**, 793 (1990).
29. B. Spengler, D. Kirsch and R. Kaufmann, *Rapid Commun. Mass Spectrom.* **5**, 198 (1991).
30. R. C. Beavis and B. T. Chait, in *Methods and Mechanisms for Producing Ions from Large Molecules*, edited by K. G. Standing and W. Ens, pp. 227–234. Plenum Press, New York (1991).
31. V. Bökelmann, B. Spengler and R. Kaufmann, *Eur. Mass Spectrom.* **1**, 81 (1995).
32. J. zhou, W. Ens, K. G. Standing and A. Verentchikov, *Rapid Commun. Mass Spectrom.* **6**, 671 (1992).
33. B. Spengler, U. Bahr, M. Karas and F. Hillenkamp, *Anal. Instrum.* **17**, 173 (1988).
34. R. Kaufmann, P. Chaurand, D. Kirsch and B. Spengler, *Rapid Commun. Mass Spectrom.* **10**, 1199 (1996).
35. R. G. Cooks, J. H. Beynon, R. M. Caprioli and G. R. Lester, *Metastable Ions*. Elsevier, Amsterdam (1973).
36. W. F. Haddon and F. W. McLafferty, *Anal. Chem.* **41**, 31 (1969).
37. B. T. Chait, *Int. J. Mass Spectrom. Ion Processes* **53**, 5115 (1982).
38. B. Sundqvist and R.D. Macfarlane, *Mass Spectrom. Rev.* **4**, 421 (1985).
39. J. Rosmarinowsky, M. Karas and F. Hillenkamp, *Int. J. Mass Spectrom. Ion Processes* **67**, 109 (1985).
40. S. Della-Negra and Y. Le Beyec, *Anal. Chem.* **57**, 2035 (1985).
41. X. Tang, W. Ens, K. G. Standing and J. B. Westmore, *Anal. Chem.* **60**, 1791 (1988).
42. B. A. Mamyrin, V. I. Karataev, D. V. Shmikk and V. A. Zagulin, *Sov. Phys. JETP* **37**, 45 (1973).
43. S. Della Negra and Y. Le Beyec, *Int. J. Mass Spectrom. Ion Processes* **61**, 21 (1984).
44. X. Tang, R. Beavis, W. Ens, F. Lafortune, B. Schueler and K. G. Standing, *Int. J. Mass Spectrom. Ion Processes* **85**, 43 (1988).
45. M. M. Cordero, T. J. Cornish, R. J. Cotter and I. A. Lys, *Rapid Commun. Mass Spectrom.* **9**, 1356 (1995).
46. P. Chaurand, B. Spengler and R. Kaufmann, presented at DESORPTION '96, Mass Spectrometry of Large Organic Ions by Electrospray, Particle and Photon Induced Desorption Ionization, Bornholm, 18–21 September, 1996.
47. P. Juhasz, M. L. Vestal and S. A. Martin, *J. Am. Soc. Mass Spectrom.* **8**, 209 (1997).
48. B. Spengler, D. Kirsch, R. Kaufmann and J. Lemoine, *J. Mass Spectrom*, **30**, 782 (1995).
49. P. Roepstorff and J. Fohlmann, *Biomed. Mass Spectrom.* **11**, 601 (1984).
50. R. S. Johnson, S. A. Martin and K. Biemann, *Int. J. Mass Spectrom. Ion Processes* **86**, 137 (1988).
51. P.-C. Liao, Z.-H. Huang and J. Allison, *J. Am. Soc. Mass Spectrom.* **8**, 501 (1997).
52. B. Spengler, F. Luetzenkirchen, S. Metzger, P. Chaurand, R. Kaufmann, W. Jeffery, M. Bartlet-Jones and D. J. C. Pappin, *Int. J. Mass Spectrom. Ion Processes* (submitted for publication).
53. B. Spengler, F. Luetzenkirchen, S. Metzger, R. Kaufmann, W. Jeffery and D. J. C. Pappin, in *Proceedings of the 44th Annual Conference on Mass Spectrometry and Allied Topics*, Portland, OR, May 13–17, 1996.
54. B. Spengler, F. Lützenkirchen and R. Kaufmann, *Org. Mass Spectrom.* **28**, 1482 (1993).
55. J. K. Eng, A. L. McCormack and J. R. Yates, III, *J. Am. Soc. Mass Spectrom.* **5**, 976 (1994).
56. M. Mann and M. Wilm, *Anal. Chem.* **66**, 4390 (1994).
57. J. Lemoine, F. Chirat and B. Domon, *J. Mass Spectrom.* **31**, 908 (1996).
58. D. J. Harvey, *J. Chromatogr. A* **720**, 429 (1996).
59. D. J. Harvey, J. David, T. J. P. Naven, B. Kuster, R. H. Bateman, M. R. Green and G. Critchley, *Rapid Commun. Mass Spectrom.* **9**, 1556 (1995).
60. P. Chaurand, R. Kaufmann, F. Lützenkirchen, B. Spengler, I. Fournier, A. Brunot, J.-C. Tabet and G. Bolbach, in *Proceedings of the 45th Annual Conference on Mass Spectrometry and Allied Topics*, Palm Springs, CA, June 1–5, 1997.
61. D. F. Hunt, R. A. Henderson, J. Shabanowitz, K. Sakaguchi, H. Michel, N. Sevilir, A. L. Cox, E. Appella and V. H. Engelhard, *Science* **255**, 1261 (1992).
62. B. Spengler, P. Bold, P. Chaurand, R. Kaufmann, H. E. Meyer, Th. Flad, C. A. Müller and H. Kalbacher, in *Proceedings of the 45th Annual Conference on Mass Spectrometry and Allied Topics*, Palm Springs, CA, June 1–5, 1997.

